Craniofacial Phenotypes of X-ray and ENU-induced Mutations in Mice

Gimara D.[a], Depew M. J.[a,b], Ragoussis J.[b], Sharpe P.[a]

[a]*Department of Craniofacial Development, Dental Institute, Kings College London, Guy's Hospital, London, UK.*
[b]*Wellcome Trust Centre for Human Genetics, University of Oxford, Oxford, UK.*

Purpose: Large scale mutagenesis screens are being used to create dominant mutations in mice that can provide new insights into gene function and enable identification of novel genes involved in particular developmental processes. The purpose of this study was to describe the craniofacial skeletal phenotypes of several mutated mouse lines generated from ethyl nitrosourea (ENU) and a combined X-ray/chemical mutagenesis in order to determine the usefulness of this approach to studying craniofacial development.

Materials and Methods: Adult mouse heads from five mutant lines were fixed and stained to reveal cartilage and bone. The skeletons were analysed in detail and compared to littermate controls.

Results: The craniofacial skeletal phenotypes of two mutant mice induced by combined chemical and X-ray treatment and three mutants from ENU treatment have been analysed. All mutations were dominant: heterozygous mice were born smaller and homozygotes were embryonic lethal. A range of phenotypes were observed, including frontonasal defects, midline asymmetries, robust ossifications and unusual suture formations.

Conclusions: The use of mutagenesis screens to produce craniofacial phenotypes from dominant gene mutations can reveal novel and unusual phenotypes not previously observed from gene knock-outs.

Key words: mutagenesis, ENU, craniofacial

Oral Biosci Med 2004; 1: 29-34 *Submitted for publication 1 September 2003; accepted for publication 27 January 2004.*

INTRODUCTION

Targeted mutagenesis in mice has provided major insights into the understanding of the genetic control of craniofacial skeletal development (Depew et al, 2001). Recently a number of large scale, random mutagenesis screens, particularly using ENU have been initiated to create more subtle and, in particular, dominant mutations in order to identify new genes involved in many different embryonic processes. These screens thus complement more traditional transgenic approaches and can provide valuable information on gene function not revealed by targeted mutagenesis. As a prelude to these large screens, smaller screens carried out by Cattanach and colleagues using both ENU and X-rays produced valuable collections of mouse mutants whose gametes have been preserved (Cattanach et al, 1989). Since many of these mutants have never been analysed in detail beyond a cursory description of their external characteristics we undertook to describe in detail the skeletal abnormalities of five mutants described as having craniofacial defects.

A total of ten mutants were investigated. Five proved to have very mild craniofacial skeletal defects and are not described here. The other five had major defects, many of which were of a nature not yet observed from gene targeting. The mutations of these five were dominant with three being ENU-induced and two from a combination of chemical (TEM+3AB) and X-ray treatments. A range of craniofacial bones was found to be affected with the most common defects being truncations of the frontonasal region. In addition, bones were observed to have increased ossification, asymmetries were observed, and unusual formations of cranial sutures were in evidence. Since the gametes from these mutants have been preserved it will be possible to identify the mutated genes responsible for the most interesting of these phenotypes and

thus provide new insights into craniofacial development based on dominant mutations that can be viewed in combination with targeted loss of gene function.

MATERIALS AND METHODS

All mice were maintained in crosses to C3H/HeHx101H F1 hybrids. Mutants 1264, 1293 and 1544 were all recovered from spermatogonial treatment with ENU. Mutants 921 and 1096 were recovered following spermatogonial exposure to a combined chemical (TEM+3AB) and X-ray treatment. Mice were sacrificed at 3-9 months and were initially fixed in 95% ethanol for two hours before removing as much tissue and skin as possible for greater penetration of bone and cartilage. The specimens were fixed for at least another four days before being treated in a solution of acetone to degrade fatty material, rinsed in water and stained in a solution containing 1 volume of 0.3% alcian blue in 70% ethanol, 0.1% alizarin red in 95% ethanol, 100% acetic acid and 17 volumes of 100% distilled autoclaved water. The skulls were then rinsed in autoclaved water before addition to a basic solution, 20% glycerol:0.2% potassium hydroxide, changing every two to three days until the skull had cleared. For storage, the skulls were transferred to 50, 80 and 100% glycerol.

RESULTS

ENU-induced Mutations

Mutant 1264: The mice were born with a flat shallow skull, 'pop-eyes', kinked tails and white feet. High proportions were born exencephalic.

The skull was smaller (shortened both rostrocaudally and mediolaterally) than normal with decreased calvarial bossing and a robust zygomatic arch. The squamosal bones presented an unusual scalloping around their sutural edges and the ethmoid bone was slightly reduced in size (Fig. 1). The palatal processes of the premaxillary bones did not extend to meet their maxillary counterparts.

Mutant 1293: The mice had craniofacial 'doming' and 'pop-eyes'. In addition, the body showed a range of bone and cartilage abnormalities and oedema.

The most noticeable cranial defects were in the frontonasal region. The nasal bones were truncated and asymmetric with enlarged concha. The nasal septum and trabecular basal plate was likewise truncated.

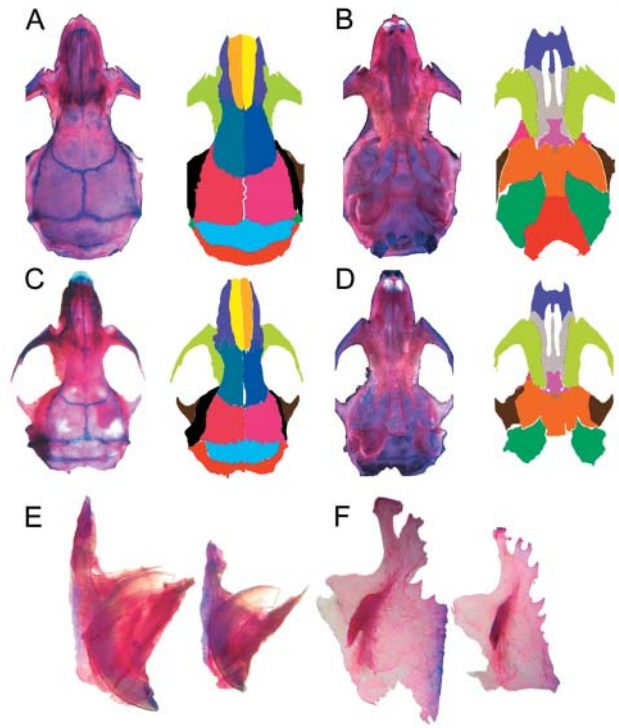

Fig. 1 A. Dorsal aspect of control. Coloured diagram to right delineates major bones. **B**. Ventral aspect of control. Coloured diagram to right delineates major bones. **C**. Dorsal aspect of ENU induced mutant 1264. Coloured diagram to right delineates major bones. **D**. Ventral aspect of ENU induced mutant 1264. Coloured diagram to right delineates major bones. **E-F**. Individual comparisons of control and ENU induced mutant 1264. **E**. Premaxilla. Note the extreme reduction in size. **F**. Lateral aspect of squamosal bones. Note the unusual exterior edges and reduced size.

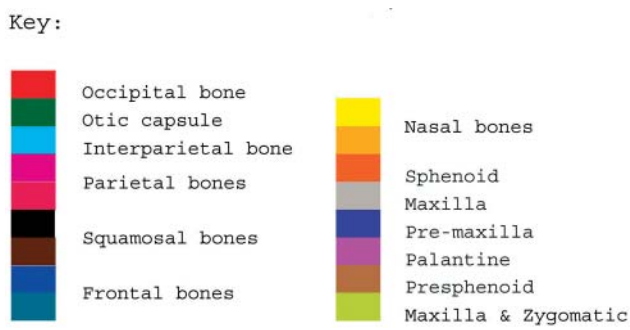

The normally serrated nasofrontal sutures were poorly defined and rounded. The frontals were shorter rostrocaudally with increased ossification along the metopic suture. Consistent with other regional defects, the ethmoid was smaller and had an unusual, asymmetric pattern to its labyrinths and connection to the vomers. The supraoccipital bone was longer, thinner and less curved while the parietals were wider. Squamosal

bones were shorter but of normal width. The tympanic bullae were reduced in size and the occipitals were wider. The sphenoids were reduced and thinner, although the pterygoid processes were more robust. It is possible that the defects observed in the caudal and temporal region were plietropic, being a consequence of those seen in the frontonasal region.

Mutant 1544: Blood spots were observed in the nasal area and the eyes bulged prominently during adulthood. Other features included bruising on the belly at birth.

The craniofacial skeletons of these mice exhibited only rather minor defects. Most notably, these included asymmetry of the frontonasal region and premaxillary palatal shelves, and convex nasals. In addition there was some reduction of the squamosal bones and reductions in size of the premaxilla and typmpanic bullae. Again, these caudal defects were possibly secondarily due to the rostral, frontonasal defects.

X-ray-induced Mutations

Mutant 921: These mice had extremely short, broad, deep heads, widely spaced eyes, and shortened nasal passages with occasional clefts. In addition, they had white feet and belly spots.

These mice had severe craniofacial skeletal abnormalities with the nasal region being the most severely affected. The skull was clearly much smaller rostrocaudally, with an asymmetric frontonasal region, and subsequently most bones were variably affected. The nasal bones were smaller and separated from each other by the presence of midline extensions from large, ectopic interfrontal bones (thus, there was no internasal suture). These interfrontal extensions pushed the nasofrontal articulations laterally. The frontal bones were greatly diminished in size and mostly separated by the caudal extensions of the ectopic interfrontals. Along the caudal end of the Metopic suture, near the nexus of the Sagittal and Coronal sutures, an ectopic, ossified nodule was observed. This nodule contained sinuses. The rostral dural attachments were, in general, abnormally ossified. Regionally, the premaxillary (e.g. smaller, lacking palatal shelves), maxillary (e.g. smaller, weakly extended palatal shelves) and ethmoid (e.g. rostrocaudally truncated, diminished and chaotically developed turbinates, and loss of the dorsoventral midline) bones were all affected.

The parietal bones were square (the Coronal suture was not curved) and smaller. The interparietal bones were slightly smaller as were the squamosals. The sphenoid occipitals were smaller as were the tympanic bullae, which were also less well defined.

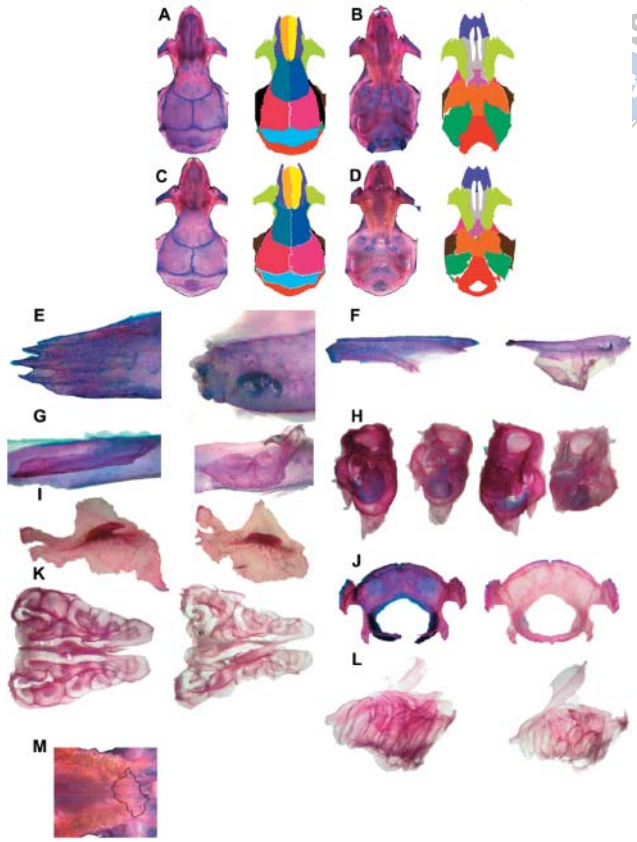

Fig. 2 A. Dorsal aspect of control. Coloured diagram to right delineates major bones. **B**. Ventral aspect of control. Coloured diagram to right delineates major bones. **C**. Dorsal aspect of ENU induced mutant 1293. Coloured diagram to right delineates major bones. **D**. Ventral aspect of ENU induced mutant 1293. Coloured diagram to right delineates major bones. **E-M**. Comparison of the individual bones of control and ENU induced mutant 1293. **E-G**. Nasal bones. **E**. Dorsal-posterior aspect. The region of the nasal bone that forms a suture with the frontal bone is scalloped and reduced in comparison to the sharp finger-like projections of the control. **F**. Lateral aspect. Nasal concha is enlarged and more curved. Exterior surface of bone is concave. **G**. Ventral aspect. Nasal concha is enlarged and more curved. **H**. Tympanic bulba. Exterior aspect. Wing reduced, blunt and straight. Its concave posterior surface also appears less developed than the control. Tympanic ring interior aspect. The reduced overall size appears more apparent in this aspect. **I**. Exterior aspect of squamosal bones. Reduced overall size. Angle between styloid process and squamous part reduced. Anterior region of squamous part blunt and less overlap with frontal bone. **J**. Occipital bone. Unlike all the other bones there is no apparent reduction in size. In fact it appears slightly larger. **K-L**. Ethmoid. **K**. Superior aspect. X-ray mutant 2 displays asymmetry of the perpendicular plate-crista galli. Unusual folding/labyrinth patterns. **L**. Lateral aspect of Ethmoid. Crista galli shows no difference in shape. Unusual folding/labyrinth patterns. **M**. Palatine. The ventral aspect of posterior palatine displays asymmetry (black line used to delineate regions of interest). In each case the mutant lies to the right or is represented alone.

Mutant 1096: These mice had very short heads, increased distances between their eyes, and shortened nasal passages. A proportion was exencephalic.

Discrete frontonasal defects were observed. The nasal bones, wider and more angular at their posterior ends, were associated with large, ectopic interfrontal bones. They had large perforations along their posterior edges, and their anterior ends were wider and flatter. The nasopremaxillary sutures were neither close nor cohesive. The premaxillary palatal shelves failed to extend caudally. An extensive ossification from the masseteric ridge into the tendon/muscle was observed. The nasal conchae were reduced in size and more cylindrical in shape with a greater angle at the posterior aspect. The nasal septum was diminished. The frontal bones were smaller and the coronal suture was straighter than normal. The parietals showed extremely abnormal ossification but were of a normal size and shape. The ethmoid was reduced in size as were the tympanic bullae.

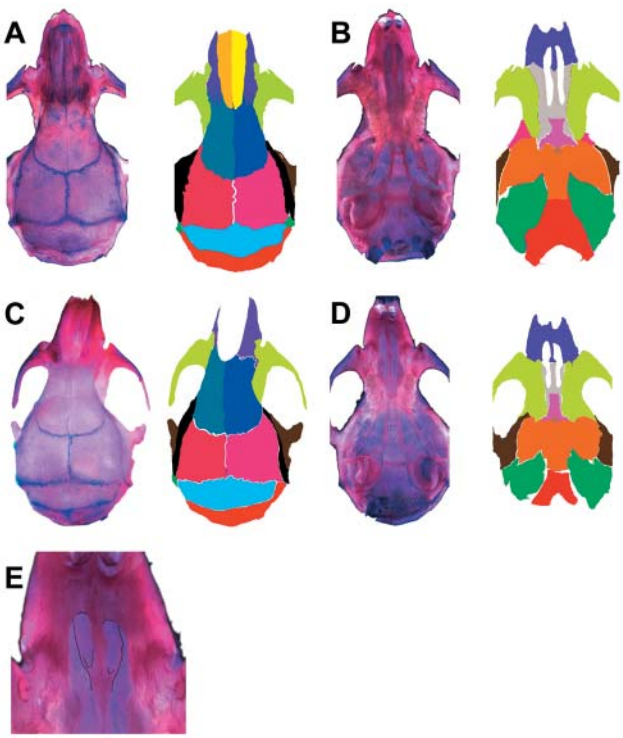

Fig. 3 A. Dorsal aspect of control. Coloured diagram to right delineates major bones. **B**. Ventral aspect of control. Coloured diagram to right delineates major bones. **C**. Dorsal aspect of ENU induced mutant 1544. Coloured diagram to right delineates major bones. **D**. Ventral aspect of ENU induced mutant 1544. Coloured diagram to right delineates major bones. **E**. Ventral aspect of anterior palatine of ENU induced mutant 1544 displays asymmetry (black line used to delineate regions of interest).

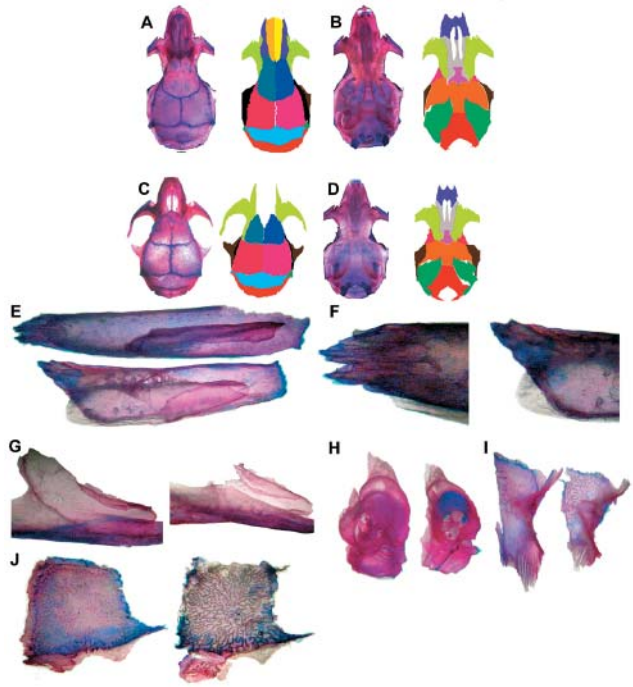

Fig. 4 A. Dorsal aspect of control. Coloured diagram to right delineates major bones. **B**. Ventral aspect of control. Coloured diagram to right delineates major bones. **C**. Dorsal aspect of X-ray-induced mutant 921. Coloured diagram to right delineates major bones. **D**. Ventral aspect of X-ray-induced mutant 921. Coloured diagram to right delineates major bones. **E-H**. Comparison of the individual bones of control vs X-ray-induced mutant 921. **E**. Dorsal aspect of nasal bones. Irregularly shaped. **F**. Superior aspect of ethmoid. Ethmoid folds/labyrinth harsh and reduced towards the median. Although truncated the inner canal and posterior is wider than the control. **G**. Ventral aspect of frontal bones. Significantly reduced and irregularly shaped towards the median of the inferior surface. Also the posterior end forms the coronal suture with the parietal bones and does not display any finger-like projections. **H**. Exterior surface of the tympanic bulla. Overall reduction in size and less developed.

DISCUSSION

In the last few years several large scale ENU mutant screens in mice, resulting in phenotypes produced from dominant mutations, have been initiated in order to identify new genes/gene functions. An aim of these screens has been to complement targeted mutagenesis and produce a more complete understanding of mouse development. An advantage of these types of screens is that they are based on phenotype, and thus the severity/importance of a particular phenotype can be assessed before attempts are made to identify the mutated gene. Moreover, since the mutations are dominant, these will provide a different kind of information

from gene targeting mutations which are predominantly recessive.

Before the initiation of the recent large-scale ENU screens, a number of interesting phenotypes were generated and catalogued at Harwell by Cattanach. Both ENU and a combination of chemical and X-ray mutagenesis strategies were used. A number of potentially interesting craniofacial phenotypes was noted based on external appearance but no detailed skeletal analyses of these mice were carried out at the time. Based on the descriptions of the craniofacial phenotypes, we selected ten mice to study the craniofacial skeleton. Our aim was to determine the nature of these craniofacial malformations and to assess the extent to which this type of random mutagenesis might produce interesting, novel phenotypes not observed with gene targeting. Five of these were found to have very subtle skeletal abnormalities. The other five had more severe phenotypes. Three ENU and two chemical/X-ray mutants were investigated; in general the ENU phenotypes were more subtle than those induced by X-rays. This is perhaps not surprising since ENU creates single base pair mutations whereas X-ray treatment creates deletions. One X-ray mutation (1096) was mapped to a deletion of chromosome 3 spanning G bands 3A3-3b.

This region is approximately 20Mbp and according to ENSEMBL data (http://www.ensembl.org/Mus_musculus/) (Fig. 6) contains 99 transcripts in the region between 18.6-36.6 Mbp that are assigned to the 3A3 and 3B chromosomal bands. Of these 41 have matches to protein or EST sequences, 25 are novel and 33 are known genes. The known genes include a number of interesting genes like Fgf2, Sox2, and a Ski-like gene. This region is homologous to the human 3q26, Xq21.3 and 4q26-27 region. Patients with deletions of 4q26-27 have craniofacial anomalies (Motegi et al, 1988; Vaux et al, 1992). Fgf2 knock out (Berk et al, 1997) are viable with no craniofacial defects reported, while SOX2 plays a role in the formation of the eye lens (Kamachi et al, 2001). One ENU mutation (1544) produced a phenotype similar to bruised (*Bru*) and the recessive mutant severe combined anaemia and thrombocytopenia (*Scat*), which is located on chromosome 8. *Bru* is an ENU induced mutation that causes a bruising about the head and hindquarters and a reduced pre-weaning viability. It is linked to a deletion of chromosome 8 involving band A1.3, named Del(8)-Bru44H (Cattanach et al, 1993). *Scat* is a recessive mutation causing intermittent episodes of severe bleeding to the homozygote. At birth the mice are pale with intradermal petechiae and bruises on exposed surfaces (Peters et al, 1990). Indeed mutant 1544 had blood spots in the nasal area and bruising on the belly at birth.

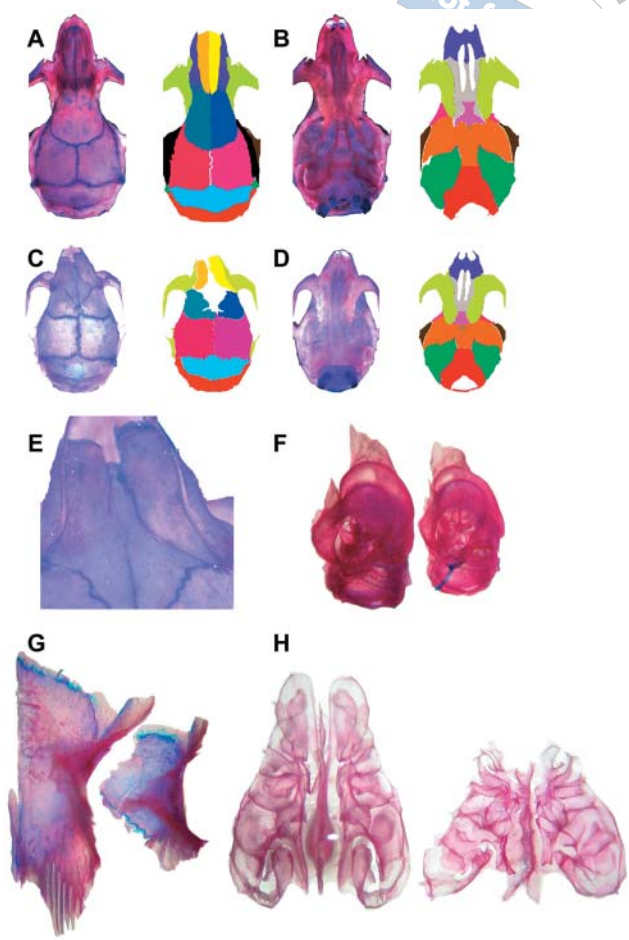

Fig. 5 A. Dorsal aspect of control. Coloured diagram to right delineates major bones. **B**. Ventral aspect of control. Coloured diagram to right delineates major bones. **C**. Dorsal aspect of X-ray-induced mutant 1096. Coloured diagram to right delineates major bones. **D**. Ventral aspect of X-ray-induced mutant 1096. Coloured diagram to right delineates major bones. Presphenoid not distinguishable. **E-I**. Comparison of the individual bones of control vs X-ray-induced mutant 1096. **E-G**. Nasal bones. **E**. Ventral aspect. Overall truncation, highly perforated and abnormal angled towards posterior end. **F**. Dorsal-posterior aspect. Lacking finger-like projections; fused. Usual shape. **G**. Lateral aspect. Reduced concha towards the posterior region. Exterior surface of bone is concave. **H**. Tympanic bones. Smaller thinner less developed structure. More cartilage present at tympanic ring. **I**. Ventral aspect of frontal bones. Wider and inferior surface more defined and extreme patterning. **J**. Parietal bones. Bone structure more extreme and defined patterning.

It is of note that the majority of the significant defects observed was in the frontonasal region. This may be due to a number of reasons. For example, this re-

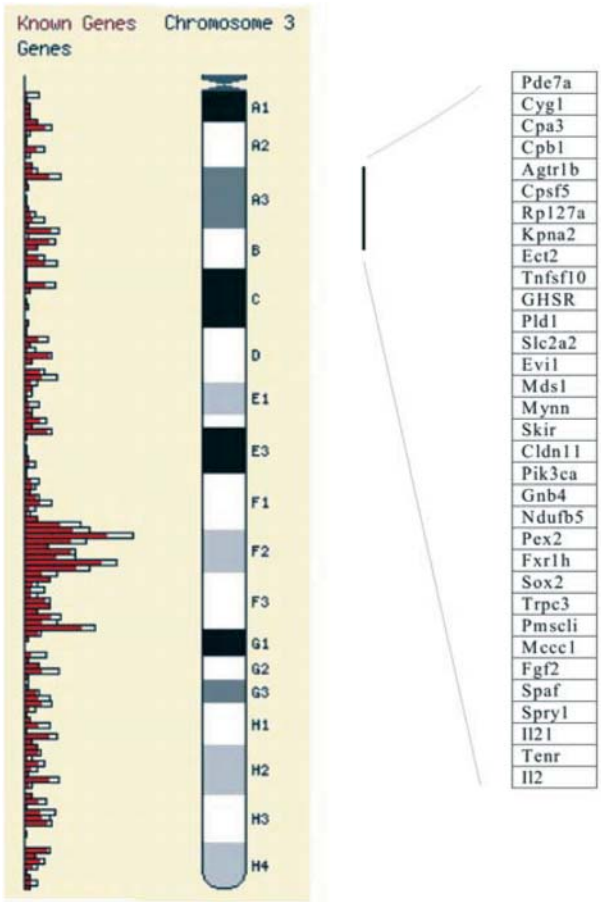

Fig. 6 Schematic diagram of mouse chromosome 3 taken from the Ensembl Genome Browser http://www.ensembl.org/Mus-musculus/mapview?chr=3 showing the extent of the deletion in MUT/1096; Del(3)79H. The region contains 33 known genes.

gion may be particularly sensitive to mutagenesis; or, that alteration of these tissues does not easily result in early lethality. It seems most likely, perhaps, that this trend toward frontonasal defects is due to selection bias: mice have extensive snouts and therefore while examining the gross anatomy of mutagenized mice it may have been easier to pick out those with highly defective snouts as having craniofacial defects. In order to understand the nature of these defects it will be essential to follow the ontogenetic progression of these phenotypes; this is particularly pertinent for the number of mutants found to have asymmetries.

X-ray-induced Mutant 921 deserves particular mention as the defects observed appear to involve both the dura and the calvarium. Both the dura mater and the intramembranous bones that form the calvarium derive from the mesenchyme of the ectomenix. Precisely how this mesenchymal population is segregated and distinctly regulated remains largely unclear. Although recent advances have been made toward understanding the molecular nature of events once a suture has developed (Depew et al, 2001), further analysis of this mutant may shed light on upstream events.

ACKNOWLEDGEMENTS

We would like to thank Bruce Cattanach (MRC Mammalian Genetics Unit, Harwell, UK) for supplying the mouse mutant samples and Oliveira Spasic-Bergovic for technical assistance. This project was funded by a grant from the Wellcome Trust.

REFERENCES

Berk M, Desai SY, Heyman HC, Colmenares C. Mice lacking the ski proto-oncogene have defects in neurulation, craniofacial, patterning, and skeletal muscle development. Genes Dev 1997;11:2029-2039.

Cattanach BM, Peters J, Rasberry C. Induction of specific locus mutations in mouse spermatogonial stem cells by combined chemical X-ray treatments. Mutat Res 1989;212:91-101.

Cattanach BM, Evans EP, Burtenshaw M, Glenister PH, Vizor L, Woodward A. Radiation-induced deletions. Mouse Genome 1993;91:853-854.

Depew M, Tucker AS, Sharpe PT. Craniofacial development. In: Rossant J, Tam PL (eds). Mouse Development. Academic Press 2001;421-498.

Kamachi Y, Uchikawa M, Tanouchi A, Sekido R, Kondoh H. Pax6 and SOX2 form a co-DNA-binding partner complex that regulates initiation of lens development. Genes Dev 2001;15:1272-1286.

Motegi T, Nakamura K, Terakawa T, Oohira A, Minoda K, Kishi K, Yanagawa Y, Hayakawa H. Deletion of a single chromosome band 4q26 in a malformed girl: exclusion of Rieger syndrome associated gene(s) from the 4q26 segment. J Med Genet 1988;25:628-630.

Okada-Ban M, Thiery JP, Jouanneau J. Fibroblast growth factor-2. Int J Biochem Cell Biol 2000;32:263-267.

Peters LL, McFarland-Starr EC, Wood BG, Barker JE. Heritable severe combined anemia and thrombocytopenia in the mouse: description of the disease and successful therapy. Blood 1990;76:745-754.

Vaux C, Sheffield L, Keith CG, Voullaire L. Evidence that Rieger syndrome maps to 4q25 or 4q27. J Med Genet 1992;29:256-258.

Reprint requests:
Paul Sharpe
Dental Institute, Kings College London
Guy's Hospital
London Bridge
London SE1 9RT
UK
E-mail paul.sharpe@kcl.ac.uk